



## OPEN

SUBJECT AREAS:  
PALAEOCLIMATE  
HYDROLOGYReceived  
22 August 2013Accepted  
10 September 2014Published  
30 September 2014Correspondence and  
requests for materials  
should be addressed to  
L.Q.C. (lqchen@soa.  
gov.cn) or R.Z.  
(ruizhang@xmu.edu.  
cn)\* These authors  
contributed equally to  
this work.

# Preliminary identification of palaeofloods with the alkane ratio $C_{31}/C_{17}$ and their potential link to global climate changes

Jianjun Wang<sup>1\*</sup>, Liqi Chen<sup>1\*</sup>, Li Li<sup>1</sup>, Jianhua He<sup>1</sup>, Jian Chen<sup>1</sup>, Chuanjie Jiang<sup>2</sup>, Weiguo Wang<sup>1</sup>, Sabrina Li<sup>3</sup>, Yiliang Li<sup>1</sup> & Rui Zhang<sup>4</sup><sup>1</sup>Third Institute of Oceanography, State Oceanic Administration (SOA), China, <sup>2</sup>Bureau of Hydrology and Water Resources Survey of Fujian Province, Fuzhou, China, <sup>3</sup>Department of Civil and Environmental Engineering, University of Waterloo, Canada, <sup>4</sup>State Key Laboratory of Marine Environmental Science, Xiamen University, Xiamen, China.

A major challenge in palaeohydrology is the extraction of continuous palaeoflood information from geophysical records. A high-resolution sediment core off the Minjiang estuary area in the Taiwan Strait, SE China, records the sedimentation history from approximately 1660 to the present. The alkane ratio  $C_{31}/C_{17}$ , a classic organic geochemical indicator of terrestrial/aquatic matter, peaks in the layers dating as 1876-1878 and 1968-1970, suggesting the large terrestrial input to the Minjiang estuary area by huge flood transporting during the each peak interval. Historical archives are consistent with this interpretations and record catastrophic floods in the Minjiang River during both intervals. Furthermore between 1876-1878 there were floods in southern China and droughts in northern China, as well as throughout Asia, Africa, Australia, and the Americas. The 1876-1878 catastrophic flood of the Minjiang River may therefore has been the local response to global climate anomalies during that time interval.

Rivers are important to the development of human societies and are the cradles of major prehistoric cultures around the world (e.g., the Huanghe River of China, the Nile River of Egypt, the Indus River of India, and the Tigris and Euphrates Rivers of Mesopotamia). Yet at the same time, extreme flooding of rivers has historically brought catastrophic devastation to human cultures. Today floods cause major losses along riversides and tributary mouths, which are commonly major political or economic centres. It is projected that the magnitudes of floods and the damage they caused will increase due to warming and precipitation anomalies related to global climate change<sup>1</sup>. In addition, flooding affects the geomorphological, ecological, and hydrological aspects of river systems. Therefore, the understanding of floods is important to both the public and science. Conventional river discharge measurements available so far, however, do not have sufficient record length to provide that understanding and, in the context of climate change, there is a growing need to include paleofloods hydrology<sup>1-5</sup>. In particular, understanding the formation mechanism, development, frequencies, and regions affected by palaeofloods is essential in helping to predict the magnitudes and recurrence intervals of modern floods<sup>4,5</sup>.

The reconstruction of ancient floods requires a combination of geomorphology, stratigraphy and sedimentology, as well as integration of historical archives<sup>1-6</sup>. Palaeoflood indicators include slackwater deposit-palaeostage indicators (SWD-PSI), the botany of floodplain vegetation, palynology, magnetic susceptibility, and sediment granulometry. Identification of SWD-PSI, combined with hydraulic flow modeling, is the most accurate method in stable-boundary fluvial reaches<sup>1,2,4</sup>. There are limitations, however, in the application of these indicators for the investigation of palaeofloods. The SWD-PSI is confined to river systems that convey sandy sediments, such as bedrock canyons<sup>1</sup>. The botany of floodplain vegetation, the palynology of floodplain sediment, the magnetic susceptibility, and the sediment granulometry, are always affected by environmental processes more complex than floods. Furthermore, quantitative information is difficult to be obtained with these indicators. Thus, extracting continuous and quantitative palaeoflood information from geophysical records is still a major challenge in palaeohydrology, and alternative indicators are needed.

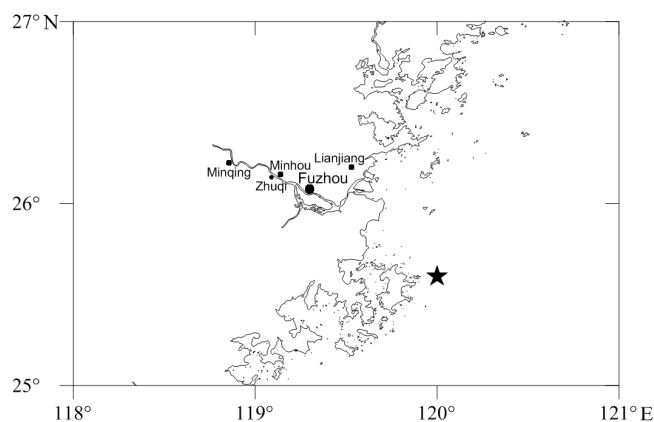


**Figure 1** | Geographical location of the sampling site and the Minjiang River (the ★ is the sampling location, and the map was created with Matlab).

Liphatic hydrocarbons are normally robust organic matter preserved in sediments, and serve as good proxies of many biogeochemical processes<sup>7,8</sup>. For example, the alkane ratio  $C_{31}/C_{17}$  is a typical organic geochemical proxy for terrestrial and aquatic input to lakes and estuarine areas<sup>9–13</sup>. The n-alkane  $C_{17}$  dominates the hydrocarbon compositions of aquatic algae and photosynthetic bacteria, and its concentrations are reflective of aquatic palaeoproductivity rates<sup>10</sup>. Vascular land plants, however, contain large proportions of  $C_{27}$ ,  $C_{29}$ , and  $C_{31}$  n-alkanes in their epicuticular waxy coatings. The relative concentration of  $C_{31}$  and  $C_{17}$  in a sediment core therefore reflects the relative input from terrestrial and aquatic sources<sup>10</sup>. Considering that floods, especially extreme floods, carry large amounts of terrestrial materials into estuaries and adjacent environments, we hypothesized that the  $C_{31}/C_{17}$  ratio might be useful as an indicator of palaeofloods.

In the present study, we analyzed the n-alkanes of a high-resolution sediment core off the estuary of Minjiang Estuary, the main river of the Taiwan Strait (Fig. 1). The comparison of the  $C_{31}/C_{17}$  pattern and the palaeofloods recorded in historical archives suggested the

$C_{31}/C_{17}$  ratio is a good geochemical proxy for palaeofloods. In addition, the local response of the floods to global climate anomalies is also discussed in this study.

## Results

**Dating of the sediment core.** The 214 cm-long sediment core was collected off the Minjiang River Estuary in the Taiwan Strait (120.0°E, 25.6°N; Fig. 1) and sectioned at intervals of 2 cm. A  $^{210}\text{Pb}$  analysis shows that the sedimentation rate of the core was  $0.61 \pm 0.07$  cm/yr (Fig. 2), which almost satisfies the assumptions of the Constant Initial Concentration model<sup>14</sup> with an exponential decrease in  $^{210}\text{Pb}$  activities up core. The relative uncertainty of the sediment age of each section is constrained within 10% (Fig. 2); thus, every 2 cm sediment layer represented  $\sim 3$  years of sedimentation. The sedimentation rate was assumed to be constant over the last 350 years due to the area's remoteness from human disturbances.

The measurement of  $^{137}\text{Cs}$  exhibited relatively low activity (less than  $10 \text{ Bq kg}^{-1}$ ) throughout the sediment core, mainly due to the shelter provided by the seawater and the location's distance from the mid-high-latitude regions of the Northern Hemisphere, where most nuclear weapons tests were performed<sup>15</sup>. The peak in  $^{137}\text{Cs}$  in the core occurred at the depth of 25 cm (Fig. 2), which was thought to be due to extensive deposition of radionuclides in the Northern Hemisphere in 1963 caused by nuclear weapons tests<sup>15–17</sup>. Consistently, the depth of 25 cm was dated as 1963–1965 by the accumulation rate of  $^{210}\text{Pb}$ .

**Distributions of n-alkanes.** The distributions of n-alkanes in the sediment core show two general patterns. The first one includes  $C_{17}$  to  $C_{33}$  alkanes, dominated by  $C_{23}$ ,  $C_{25}$  and  $C_{27}$ , whereas the second one shows almost no long-chain n-alkanes, with  $C_{17}$  and  $C_{18}$  being dominant (Fig. 3). Because the sources of  $C_{21}$ ,  $C_{23}$  and  $C_{25}$  are more complex and might be contributed by aquatic macrophytes<sup>7,18,19</sup>, we did not use these n-alkanes as terrestrial indicators. Significant correlations of various classic biomarkers (e.g.,  $C_{27}$ ,  $C_{29}$ , and  $C_{31}$  n-alkanes) were observed (the linear regression,  $R^2$ , was 0.79 for  $C_{31}$  and  $C_{29}$ , 0.59 for  $C_{31}$  and  $C_{27}$ , and 0.87 for  $C_{29}$  and  $C_{27}$ ;  $P < 0.01$ ), indicating the dominant sources of these n-alkanes are indeed terrestrial. The ratio of  $C_{31}/C_{17}$  was applied to

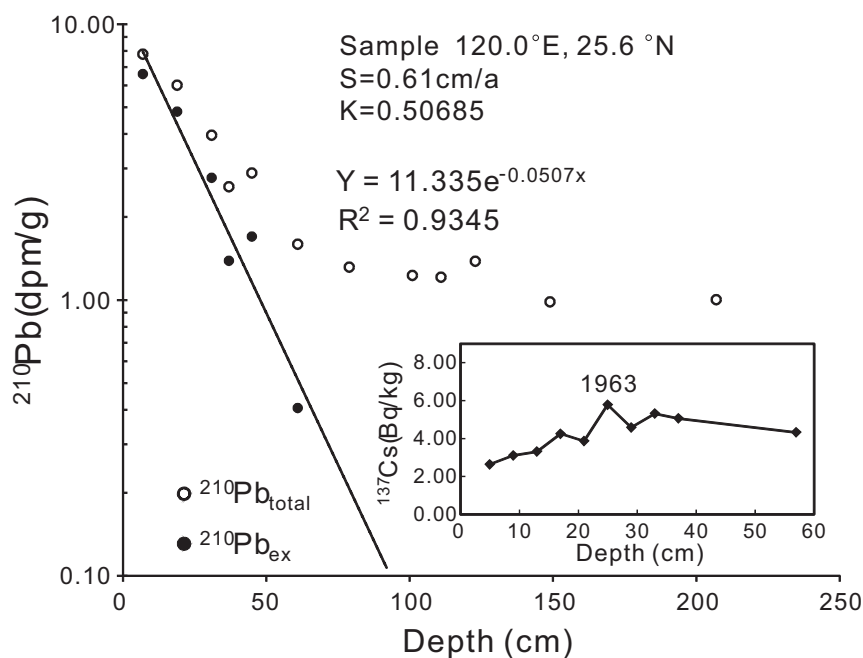


**Figure 2** |  $^{210}\text{Pb}$  and  $^{137}\text{Cs}$  (inset) dating of the sediment core collected from the Taiwan Strait. The sedimentation rate determined by  $^{210}\text{Pb}$  analyses and the peak of  $^{137}\text{Cs}$  activity (dated as 1963) are shown.

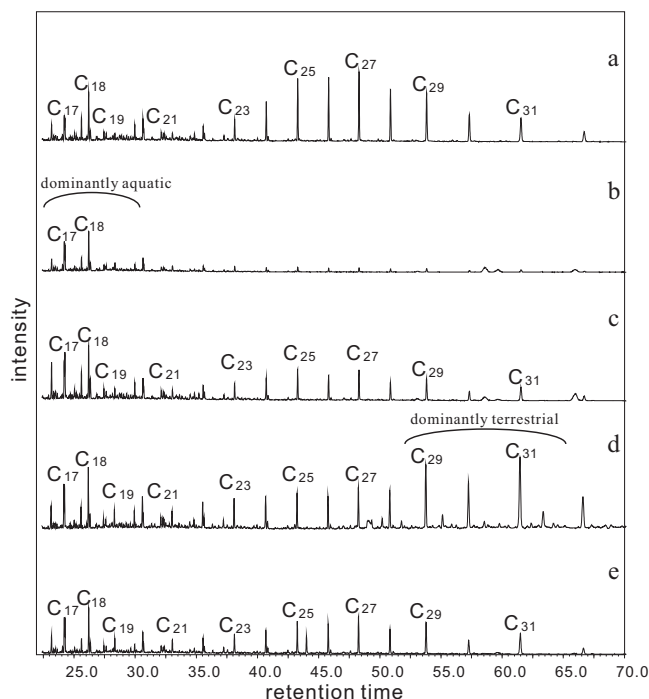


**Figure 3** | Representative patterns of n-alkane distribution in the sediment core (mass to charge ratio:  $M/Z$  57) (a: 75 cm; b: 107 cm; c: 21 cm, the layer following the flood; d: 23 cm, the flood layer of 1968–1970; e: 25 cm, the layer preceding the flood).

evaluate the relative contribution of terrestrial and marine input to the sedimentation of the Minjiang River Estuary.

The discrepancies in the alkane distribution in different sediment layers (Fig. 3) cause a zigzagging  $C_{31}/C_{17}$  trend in the sediment core (Fig. 4). Most of the  $C_{31}/C_{17}$  values ranged from 0.1 to 3.5. The entire trend of the maximum of the  $C_{31}/C_{17}$  ratio decreases ( $P < 0.01$ ), with the exception of two peaks, a maxima of 5.3 in 1876–1878, and another of 5.6 in 1968–1970. The n-alkane distribution pattern of the 1968–1970 sample, as well as the samples preceding and following this sample, is shown in Fig. 3, illustrating that the abrupt increase in  $C_{31}/C_{17}$  in 1968–1970 was due to the increased amount of  $C_{31}$  n-alkanes in this layer.

## Discussion

Fluvial delivery and aeolian transport are the two main modes of terrestrial input of biomarkers into marine sediments. Fluvial delivery is the main transportation mechanism for coastal areas, and wind is dominant for the open oceans<sup>20</sup>. In the case of our sampling site, the estuary of the Minjiang River, the main mechanism by which biomarkers and other organic matter are delivered is certainly fluvial processes. Therefore, the pattern of n-alkanes in our sampling site should be influenced by two major factors: 1) the vegetation coverage of the drainage area, and 2) variations in runoff into the Minjiang River.

Although the historical records of the vegetation coverage of the Minjiang River drainage area over the past hundred years are not complete, there is little doubt that the river's catchment area has been intensely impacted by human activities, such as deforestation, land reclamation and construction. Increasing economic development and population growth reduced the vegetation coverage, and the consistently decreasing vegetation coverage which in turn affected the terrestrial input into the estuary area. Alternatively, a reduction of precipitation resulted in reduced river discharge, as well as terrestrial input, to the estuarine area. Annual precipitation time series for Fuzhou (the capital of Fujian Province and the biggest city located

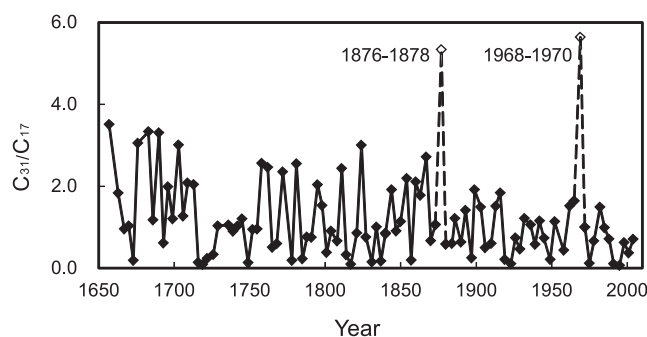


**Figure 4** | The  $C_{31}/C_{17}$  trend in the sediment core over the past 350 years. The maxima in 1876–1878 and 1968–1970 are indicated.

along the lower Minjiang River) exhibit a progressively decreasing trend from 1900–1999<sup>21</sup>. This pattern is also supported by the sediment yield record at the Zhuqi Hydrometric Station (26.09°E, 119.06°N), which showed a generally decreasing trend from 1963 to 2006 (Supplementary Information Fig. S1). Therefore, the decrease in vegetation coverage, precipitation and discharge is therefore consistent with the overall decreasing trend in the ratio of  $C_{31}/C_{17}$  in the sediment core.

Because there were low possibilities that the vegetation coverage would increase rapidly within a short period, the amount of precipitation and discharge might be the main causes of the  $C_{31}/C_{17}$  peaks observed in the 1876–1878 and 1968–1970 samples (Fig. 4). The historical chronicles of Fuzhou and other cities (Minhou, Minqing and Lianjiang; Fig. 1) located along the Minjiang River documents catastrophic floods in 1876–1878 and 1968<sup>22,23</sup>. The flood that occurred in 1968 was recorded as a hundred-year flood. Hydrological records documented that on June 19<sup>th</sup>, 1968, the maximum water level in the Minjiang River at Yanfumen Pier was 15 m above the average, and the measured flow rate was 23,800 m<sup>3</sup>/s at the Shilian hydrometric station and 29,400 m<sup>3</sup>/s at the Zhuqi hydrometric station. According to other records of Fujian Province, heavy rainstorms also occurred in the cities of Lianjiang, Minqing, and Minhou in June 1968<sup>22</sup>.

The floods that occurred in the Minjiang River in 1876–1878 are also recorded in the historic chronicles of Fuzhou, Minhou, Minqing and Lianjiang: “Since the Qing Dynasty, floods were frequent in Fuzhou City. The floods in 1875 AD, 1876 AD were the most severe floods. From May 16<sup>th</sup> to the 19<sup>th</sup> in year 1875, heavy rainstorms impacted Fuzhou City all day and night. Moreover in 1876, the county of Minqing suffered from a heavy rainstorm which had devastating effects. A massive surge ran down the Minjiang River and flooded the city at an average height of more than 10 m. The whole city was overwhelmed from this unexpected event which resulted in huge population losses<sup>22</sup>.”

Total organic carbon (TOC) and magnetic susceptibility (MS) have been used as palaeoflood proxies in riverine sediment cores<sup>24,25</sup>. Our analysis showed that the TOC content in the sediment core varied from 0.58% to 1.03% without clear temporal variations and with no indication of any palaeoflood events (Supplementary Information Fig. S2). The production and sedimentation of total organic matter is mainly contributed by marine primary producers for our sampling site, which is a typical marine environment. This condition might lead to the constant pattern of TOC in our sediment core. Similarly, the MS trend of our sediment core did not match the pattern of the  $C_{31}/C_{17}$  ratio (Supplementary Information Fig. S3). Previous studies suggested that the MS of the sediments in marine environments is impacted by ecological or geological processes, such as the MS of sedimentation particles, the ocean current, and the oxidation/reduction conditions<sup>26,27</sup>. Therefore, we suggest that the TOC, MS and colour of the sediment might be more applicable as



flood proxies in riverine environments. The  $C_{31}/C_{17}$  ratio, as proposed in this study, might work better as a palaeoflood proxy for marine sediment cores because of its high sensitivity to terrestrial input.

However, detailed investigation of the controls of preservation of  $C_{31}$  and  $C_{17}$  alkanes are needed for their application in different sedimentary environments. Degradation or alteration may occur after the alkanes are buried into sediment, which is extensive in the oxic environments and bioturbated surface layer of sediment<sup>8,28</sup>. For our sampling site, the relatively rapid sedimentation rate reduced the residence time of alkanes in oxic and bioturbated layers, developing a better preservation conditions. As illustrated in Figure 3,  $C_{31}$ , not  $C_{17}$  is the major cause for the variations of  $C_{31}/C_{17}$  in our sediment core. This suggested that degradation or alteration of alkanes did not affect their indication of paleoenvironments.

Despite the advantages of the  $C_{31}/C_{17}$  ratio relative to other palaeoflood indicators, more data (such as more sediment cores or over-bank deposits on floodplains or levees) are required to confirm its application on larger spatial and temporal scales. In addition, palaeoflood events may be missed by our technique because of the resolution limitations of the sedimentation or the synchronous occurrences of flood and drought. According to a field investigation conducted by Luo (1987)<sup>29</sup>, there was a flood in 1909 in the Minjiang River. We also found reference to this flood during our own historical literature survey<sup>22</sup>. However, the  $C_{31}/C_{17}$  ratio showed no evidence of this event (Fig. 4). We suggest that this discrepancy might due to the large droughts that occurred in the same year and the subsequent two years<sup>22</sup>. Because the resolution of our sediment core is 0.61 cm/yr and the sediment core was sampled at 2 cm intervals, droughts during the 3 years following a flood might obliterate the  $C_{31}/C_{17}$  signal from the flood by reducing the vegetation and thus the terrestrial  $C_{31}$  alkane input.

The climate is the principal driving force for hydrologic systems. The floods occurring between 1876 and 1878 in the Minjiang River documented a local response to global climate anomalies. The period 1876–1878 was near the end of the Little Ice Age, when the climate had begun to gradually warm. During this transition, climatic extremes were more frequent in China and throughout the world<sup>30,31</sup>. Historical records document the occurrence of several heavy rainstorms in southern China (e.g., Taiwan, Guangdong, etc.), which may be linked to the occurrence of floods<sup>6</sup>. At the same time, a great drought and famine took place in northern China, which lasted for four years from 1875 to 1878<sup>30,31</sup>. This was the most severe drought of the Qing Dynasty, known as the Great Drought and Famine of JinYu (Shanxi and Hebei Provinces of China). During this same period, the winters were extremely cold throughout China<sup>6,31</sup>. In addition, droughts were common worldwide, and several severe droughts were observed in parts of Asia, Africa, South and North America, Europe and Australia<sup>32–35</sup>. The sunspot data from the National Geophysical Data Center<sup>36</sup> show that the solar activity from 1875–1879 AD was at a low level, which would weaken the intensity of Hadley cell circulation<sup>36,37</sup>. Furthermore, the ENSO signal in 1877 was one of the strongest in the past 450 years<sup>32,38–40</sup>. The failure of the Asian Monsoon and sea surface temperature anomalies have also been used to explain the climate changes of 1876–1878<sup>32,33</sup>. A combination of anomalies in atmospheric thermodynamic and hydrodynamic circulation are likely the main cause of the global climate extremes experienced during the years 1876–1878. The palaeoflood of the Minjiang River in 1876–1878 observed in our study provides an important archive of the abrupt changes in global climate and their impact on local hydrological cycles.

In summary, our study demonstrates for the first time the match between the peaks of the n-alkane  $C_{31}/C_{17}$  ratio and the historical flood records of the Minjiang River in 1968 and 1876–1878. This result suggested the application of the  $C_{31}/C_{17}$  ratio, a classic organic geochemical indicator of terrestrial/aquatic matter, as a potential

proxy for identifying the occurrence of palaeofloods in marine deposits, especially where other palaeoflood indicators are difficult to obtain.

## Methods

**Sampling.** The 214 cm-long sediment core B837 was collected in the Taiwan Strait off the Minjiang River Estuary (120.0°E, 25.6°N). The Minjiang River is important in south-eastern China with a catchment area of 60,092 km<sup>2</sup> and a discharge of  $6.2 \times 10^{10}$  km<sup>3</sup> per year. The colour of the sediment was mainly greyish green. The sediment core B837 was sectioned at intervals of 2 cm for further analysis.

**<sup>210</sup>Pb dating.** <sup>210</sup>Pb analysis was performed on 12 samples down the sediment profile (at depths of 7, 19, 31, 37, 45, 61, 79, 101, 111, 123, 149, and 207 cm) in the sediment profile. The <sup>210</sup>Pb content was measured via the daughter product nuclide <sup>210</sup>Po using the standard radiochemical procedure after auto-deposition on a silver planchet. Approximately 2 to 3 g of powdered material was completely dissolved in HF, HClO<sub>4</sub>, HNO<sub>3</sub>, and HCl in a Teflon vessel. The polonium isotopes (<sup>209</sup>Po and <sup>210</sup>Po) were detected using an Alpha spectrometer (7200-08, Canberra, USA). The analyses were performed at the Marine Radioactive Laboratory of the Third Institute of Oceanography, State Oceanic Administration, Xiamen, China.

**<sup>137</sup>Cs dating.** To establish the chronology of the core, the specific activities of <sup>137</sup>Cs in 10 subsamples (at depths of 5, 9, 13, 17, 21, 25, 29, 33, 37 and 57 cm) were measured. The samples were counted with an ultra-low background HPGe gamma spectrometer (Canberra BE6530, USA). The <sup>137</sup>Cs was quantified by the 662 keV photopeak. The LabSOCs (Laboratory Sourceless Calibration Software) was used for efficiency calibration of the counts. This analytical process allowed us to measure <sup>137</sup>Cs with a detection limit of 0.71 Bq kg<sup>-1</sup> dry sediment (count time: 1 day) and a measurement precision of between approximately ±22% and ±43% at the 95% level of confidence.

**n-Alkane analysis.** For the organic biomarker analysis, freeze-dried sediment samples were Soxhlet extracted for 72 h with 2 : 1 dichloromethane/methanol. The extracts were concentrated using rotary evaporation and then saponified using 0.5 M KOH/MeOH. The neutral lipids were partitioned out of the basic solution with hexane and further separated using (5% deactivated) silica gel column chromatography and solvents of increasing polarity from hexane to methylene chloride. The alkane fraction was eluted and obtained in the hexane solvent.

This alkane fraction was analysed in an HP 5890 gas chromatograph-mass spectrometer with a DB-5 ms (50 m × 0.32 mm and 0.25 μm film thickness) capillary column (J&W). Helium was used as the carrier gas. The mass spectrometer was operated in EI mode at 70 eV. The MS data were acquired in the full mode and processed using the Chemstation data system. The GC oven for alkanes was programmed as follows: held for 2 min at 60°C, increased to 200°C at 7°C/min, then increased to 280°C at 3°C/min, and finally held for 30 min at 280°C.

- Baker, V. R. Palaeoflood hydrology in a global context. *Catena* **66**, 161–168 (2006).
- Baker, V. R. Paleoflood hydrology: Origin, progress, prospects. *Geomorphology* **101**, 1–13 (2008).
- Knox, J. C. Sensitivity of modern and Holocene floods to climate change. *Quat. Sci. Rev.* **19**, 439–457 (2000).
- Kochel, R. C. & Baker, V. R. Paleoflood hydrology. *Science* **215**, 353–361 (1982).
- Saint-Laurent, D. Palaeoflood hydrology: an emerging science. *Prog. Phys. Geog.* **28**, 531–543 (2004).
- Song, H., Gao, J., Sun, G. & Zhang, B. *The historical record of the climate extremes in ancient China*. (The Education Press of Anhui, Hefei, 2002).
- Cranwell, P. Lipid geochemistry of sediments from Upton Broad, a small productive lake. *Org. Geochem.* **7**, 25–37 (1984).
- Meyers, P. A. Organic geochemical proxies of paleoceanographic, paleolimnologic, and paleoclimatic processes. *Org. Geochem.* **27**, 213–250 (1997).
- González-Vila, F. J., Polvillo, O., Boski, T., Moura, D. & de Andrés, J. R. Biomarker patterns in a time-resolved Holocene/terminal Pleistocene sedimentary sequence from the Guadiana river estuarine area (SW Portugal/Spain border). *Org. Geochem.* **34**, 1601–1613 (2003).
- Meyers, P. A. Applications of organic geochemistry to paleolimnological reconstructions: a summary of examples from the Laurentian Great Lakes. *Org. Geochem.* **34**, 261–289 (2003).
- Préndez, M., Barra, C., Toledo, C. & Richter, P. Alkanes and polycyclic aromatic hydrocarbons in marine surficial sediment near Antarctic stations at Fildes Peninsula, King George Island. *Antarct. Sci.* **23**, 578–588 (2011).
- Qu, W. *et al.* Evidence for an aquatic plant origin of ketones found in Taihu Lake sediments. *Hydrobiologia* **397**, 149–154 (1999).
- Ratnayake, N. P., Suzuki, N., Okada, M. & Takagi, M. The variations of stable carbon isotope ratio of land plant-derived n-alkanes in deep-sea sediments from the Bering Sea and the North Pacific Ocean during the last 250,000 years. *Chem. Geol.* **228**, 197–208 (2006).
- Kirchner, G. <sup>210</sup>Pb as a tool for establishing sediment chronologies: examples of potentials and limitations of conventional dating models. *J. Environ. Radioact.* **102**, 490–494 (2011).



15. Chen, B. *et al.* Radionuclide dating of recent sediment and the validation of pollen-environment reconstruction in a small watershed reservoir in southeastern China. *Catena* **115**, 29–38 (2014).
16. Benoit, G. & Rozan, T. F.  $^{210}\text{Pb}$  and  $^{137}\text{Cs}$  dating methods in lakes: a retrospective study. *J. Paleolimnol.* **25**, 455–465 (2001).
17. Klaminder, J., Appleby, P., Crook, P. & Renberg, I. Post-deposition diffusion of  $^{137}\text{Cs}$  in lake sediment: Implications for radiocaesium dating. *Sedimentology* **59**, 2259–2267 (2012).
18. Ficken, K., Li, B., Swain, D. & Eglinton, G. An n-alkane proxy for the sedimentary input of submerged/floating freshwater aquatic macrophytes. *Org. Geochem.* **31**, 745–749 (2000).
19. Weller, P. & Stein, R. Paleogene biomarker records from the central Arctic Ocean (Integrated Ocean Drilling Program Expedition 302): Organic carbon sources, anoxia, and sea surface temperature. *Paleoceanography* **23** (2008).
20. Pancost, R. D. & Boot, C. S. The palaeoclimatic utility of terrestrial biomarkers in marine sediments. *Mar. Chem.* **92**, 239–261 (2004).
21. Zhu, Y. & Shi, N. Analysis on the statistical characteristics of Fuzhou annual precipitation time series during the past one hundred years *Hydrology. (China)* **22**, 22–25 (2002).
22. The Chorography Committee of Fujian. *The Chorography of Fujian, China*. (Fangzhi Press, Beijing, 2002).
23. Central Hydrological Station of Fujian Province. The summary of flood of Minjiang River in June, 1968. *Hydrology (China)* **4**, 53–57 (1981).
24. Brown, S. L., Bierman, P. R., Lini, A. & Southon, J. 10000 yr record of extreme hydrologic events. *Geology* **28**, 335 (2000).
25. Zhu, C. *et al.* Identifying paleoflood deposits archived in Zhongba Site, the Three Gorges reservoir region of the Yangtze River, China. *Chin. Sci. Bull.* **50**, 2493–2504 (2005).
26. Ludwig, P. *et al.* Characterization of primary and secondary magnetite in marine sediment by combining chemical and magnetic unmixing techniques. *Global Planet. Change* **110**, 321–339 (2013).
27. Zhou, X., Sun, L., Huang, W., Cheng, W. & Jia, N. Precipitation in the Yellow River drainage basin and East Asian monsoon strength on a decadal time scale. *Quat. Res.* **78**, 486–491 (2012).
28. Jeng, W.-L. & Huh, C.-A. A comparison of sedimentary aliphatic hydrocarbon distribution between the southern Okinawa Trough and a nearby river with high sediment discharge. *Estua. Coast Shelf Sci.* **66**, 217–224 (2006).
29. Luo, C. Z. Investigation and regionalization of historical floods in China. *J. Hydrol.* **96**, 41–51 (1987).
30. Hao, Z. X., Zheng, J. Y., Wu, G. F., Zhang, X. Z. & Ge, Q. S. 1876–1878 severe drought in North China: Facts, impacts and climatic background. *Chin. Sci. Bull.* **55**, 3001–3007 (in Chinese with English abstract) (2010).
31. Zhang, D. & Liang, Y. A long lasting and extensive drought event over China during 1876–1878. *Adv. Climate Change Res.* **6**, 106–112 (in Chinese with English abstract) (2010).
32. Charles, C. D., Hunter, D. E. & Fairbanks, R. G. Interaction between the ENSO and the Asian monsoon in a coral record of tropical climate. *Science* **277**, 925–928 (1997).
33. Herweijer, C., Seager, R. & Cook, E. R. North American droughts of the mid to late nineteenth century: a history, simulation and implication for Mediaeval drought. *Holocene* **16**, 159–171 (2006).
34. Kiladis, G. N. & Diaz, H. F. An analysis of the 1877–78 ENSO episode and comparison with 1982–83. *Monthly Weather Review* **114**, 1035–1047 (1986).
35. Nicholls, N. Historical El Niño/Southern oscillation variability in the Australasian region. *El Niño historical and paleoclimatic aspects of the Southern Oscillation*. (eds. Diaz H F & M. V ) 151–173 (Cambridge University Press, Cambridge, 1992).
36. NGDC NOAA, The yearly sunspot number dataset, [ftp://ftp.ngdc.noaa.gov/STP/space-weather/solar-data/solar-indices/sunspot-numbers/international/listings/listing\\_international-sunspot-numbers\\_yearly.txt](ftp://ftp.ngdc.noaa.gov/STP/space-weather/solar-data/solar-indices/sunspot-numbers/international/listings/listing_international-sunspot-numbers_yearly.txt). (Date of access: 28/05/2014).
37. Wang, J. The other side of climate changes—A second opinion on CO<sub>2</sub> and global warming. *Bull. Chin. Acad. Sci.* 438–447 (in Chinese with English Abstract) (2010).
38. Yan, H. *et al.* A record of the Southern Oscillation index for the past 2,000 years from precipitation proxies. *Nat. Geosci.* **4**, 611–614 (2011).
39. Cook, E. R. *et al.* Asian monsoon failure and megadrought during the last millennium. *Science* **328**, 486–489 (2010).
40. Quinn, W. H., Neal, V. T. & De Mayolo, S. E. A. El Niño occurrences over the past four and a half centuries. *J. Geophys. Res.* **92**, 14449–14461 (1987).

## Acknowledgments

This work was supported by the NSFC project (41106168, 41376132, 41230529), the SOA project (2004DIB5J178) and the Fundamental Research Funds for the Central Universities (2012121052). L.L. was supported by the 973 program (2009CB421205). Prof. John Hodgkiss of the University of Hong Kong is thanked for his help with English.

## Author contributions

J.W., L.C. and R.Z. conceived the study, designed and performed the experiment, analysed the data and wrote the manuscript. L.L., J.H., J.C., C.J., W.W., Y.L. and S.L. provided assistance during the experiment and data analysis as well as comments for this manuscript.

## Additional information

**Supplementary information** accompanies this paper at <http://www.nature.com/scientificreports>

**Competing financial interests:** The authors declare no competing financial interests.

**How to cite this article:** Wang, J. *et al.* Preliminary identification of palaeofloods with the alkane ratio C<sub>31</sub>/C<sub>17</sub> and their potential link to global climate changes. *Sci. Rep.* **4**, 6502; DOI:10.1038/srep06502 (2014).



This work is licensed under a Creative Commons Attribution-NonCommercial-ShareAlike 4.0 International License. The images or other third party material in this article are included in the article's Creative Commons license, unless indicated otherwise in the credit line; if the material is not included under the Creative Commons license, users will need to obtain permission from the license holder in order to reproduce the material. To view a copy of this license, visit <http://creativecommons.org/licenses/by-nc-sa/4.0/>